Solid-State ^{13}C NMR Study of Tyrosine Protonation in Dark-Adapted Bacteriorhodopsin†

J. Herzfeld,§ S. K. Das Gupta,‡ M. R. Farrar,‡,§ G. S. Harbison,‡,∥ A. E. McDermott,‡ S. L. Pelletier,§ D. P. Raleigh,‡,⊥ S. O. Smith,‡,# C. Winkel,° J. Lugtenburg,° and R. G. Griffin*,‡

Francis Bitter National Magnet Laboratory and Department of Chemistry, Massachusetts Institute of Technology, Cambridge, Massachusetts 02139, Department of Chemistry, Brandeis University, Waltham, Massachusetts 02254-9110, and Department of Chemistry, Rijksuniversiteit te Leiden, 2300 RA Leiden, The Netherlands

Received August 28, 1989; Revised Manuscript Received February 21, 1990

ABSTRACT: Solid-state ^{13}C MAS NMR spectra were obtained for dark-adapted bacteriorhodopsin (bR) labeled with [4′-^{13}C]Tyr. Difference spectra (labeled minus natural abundance) taken at pH values between 2 and 12, and temperatures between 20 and −90 °C, exhibit a single signal centered at 156 ppm, indicating that the 11 tyrosines are protonated over a wide pH range. However, at pH 13, a second line appears in the spectrum with an isotropic shift of 165 ppm. Comparisons with solution and solid-state spectra of model compounds suggest that this second line is due to the formation of tyrosinate. Integrated intensities indicate that about half of the tyrosines are deprotonated at pH 13. This result demonstrates that deprotonated tyrosines in a membrane protein are detectable with solid-state NMR and that neither the bR_{568} nor the bR_{555} form of bR present in the dark-adapted state contains a tyrosinate at pH values between 2 and 12. Deprotonation of a single tyrosine in bR_{568} would account for 3.6% of the total tyrosine signal, which would be detectable with the current signal-to-noise ratio. We observe a slight heterogeneity and subtle line-width changes in the tyrosine signal between pH 7 and pH 12, which we interpret to be due to protein environmental effects (such as changes in hydrogen bonding) rather than complete deprotonation of tyrosine residue(s).

Bacteriorhodopsin (bR),[1] the sole protein found in the purple patches of the cell membrane of *Halobacterium halobium*, functions as a light-driven proton pump (Oesterhelt & Stoeckenius, 1973). A retinal chromophore, linked to Lys-216 by a protonated Schiff base (Bayley et al., 1981), imparts the characteristic purple color. Motivated by its importance as a member of the rhodopsin family and as an ion pump, and encouraged by its availability and stability, bR has been the focus of intense experimental scrutiny [for recent reviews, see Stoeckenius and Bogomolni (1982), Stockburger et al. (1986), and Terner and El-Sayed (1985)]. Chemical (Pettei et al., 1977), resonance Raman (Lewis et al., 1974; Braiman & Mathies, 1980, 1982; Smith et al., 1984, 1985), FTIR (Argade & Rothschild, 1983; Rothschild et al., 1982; Bagley et al., 1982), and solid-state NMR (Harbison et al., 1983, 1984a,b, 1985a; Smith et al., 1989b) studies have shown that dark-adapted bR comprises a mixture of bR_{555}[2] and bR_{568} containing, respectively, 6-s-trans,13-cis,15-syn and 6-s-trans,13-trans,15-anti protonated Schiff base retinal chromophores. The functional light-adapted state contains only bR_{568} (Oesterhelt & Stoeckenius, 1974; Pettei et al., 1977; Scherrer et al., 1989). After absorption of a photon, a K intermediate is rapidly formed (<10 ps) by isomerization about the 13=14 double bond (Tsuda et al., 1980; Hsieh et al., 1981; Braiman & Mathies, 1982). This proceeds to the L intermediate, which subsequently deprotonates to form the M state (Lewis et al., 1974; Smith et al., 1983). Reprotonation and 13-cis to all-trans isomerization regenerate the bR_{568} state.

Many features of the structure of the retinal chromophore in these intermediates are well understood. However, the goal of understanding proton pumping remains elusive, largely because the structure and role of the protein in the photocycle have not been characterized. The ionizable amino acids are expected to be important participants in proton transfer. Of the acidic amino acids, the most acessible for spectroscopic purposes has been tyrosine, which possesses a characteristic UV absorption for optical studies and is easily isotopically labeled for FTIR and NMR studies. An ionized tyrosine could act as the Schiff base counterion or interact with other parts of the chromophore. Tyrosines and tyrosinates have also been placed in the putative proton wire (Nagle & Morowitz, 1978; Nagle & Tristan-Nagle, 1983; Nagle, 1987; Zundel, 1988), which is proposed to conduct protons between the Schiff base and the membrane surfaces.

Several techniques have been utilized to detect the presence of tyrosinates at various stages of the bR photocycle. In many cases the results are inconsistent with one another. Some UV spectroscopic investigations show evidence for deprotonation

† This research was supported by the National Institutes of Health (GM-23289, GM-36810, and RR-00995), the Netherlands Foundation for Chemical Research (SON), and the Netherlands Organization for the Advancement of Pure Science (NWO). M.R.F. and A.E.M. are supported by American Cancer Society Postdoctoral Fellowships (PF-3114 and PF-3283, respectively). S.O.S. was supported by a USPHS Postdoctoral Fellowship (GM-10502).

§ Brandeis University.

‡ Massachusetts Institute of Technology.

∥ Present address: Department of Chemistry, State University of New York at Stony Brook, Stony Brook, NY 11794-3400.

⊥ Present address: Inorganic Chemistry Laboratory, Oxford University, South Parks Road, Oxford OX1 3QR, England.

Present address: Department of Molecular Biophysics and Biochemistry, Yale University, New Haven, CT 06511.

° Rijksuniversiteit te Leiden.

[1] Abbreviations: bR, bacteriorhodopsin; bR_{568}, all-trans component of dark-adapted bacteriorhodopsin; bR_{555}, 13-cis component of dark-adapted bacteriorhodopsin;[2] MAS, magic angle spinning; NMR, nuclear magnetic resonance; FTIR, Fourier transform infrared; BPTI, bovine pancreatic trypsin inhibitor; Tyr, tyrosine; Lys, lysine; TMS, tetramethylsilane.

[2] Scherrer et al. (1989) have remeasured the absorption maximum of the 13-cis component of dark-adapted bR and found it to have a maximum at 555 nm rather than 548 nm. For that reason we will now use the new notation of bR_{555} rather than the old convention of bR_{548}.

0006-2960/90/0429-5567$02.50/0

of a tyrosine in the bR to M transition (Becher et al., 1978; Bogolmoni et al., 1978, 1980; Hess & Kuschmitz, 1979; Fukumoto et al., 1984), and kinetic studies, monitoring UV and visible absorbance, indicate a pH dependence of the rate of formation of M that is attributed to the pK_a of a tyrosine residue (Rosenbach et al., 1982; Kalisky et al., 1981; Fukumoto et al., 1984). Subsequent UV studies, however, found that deprotonation of a tyrosine lags slightly behind the formation of M (Hanamoto et al., 1984) and that the rate of M formation is independent of pH. Scherrer and Stoeckenius (1984, 1985) suggested that it is not the rate of M formation that depends on pH but rather the varying amount of each of two types of M, a fast-forming and a slow-forming species, which accounts for the apparent pH dependence.

In all of the above UV experiments, light- or dark-adapted bR was photoactivated, and a tyrosinate was seen to appear on a time scale roughly proximal to that of M formation. The experiments, all of which were sensitive to the formation of a tyrosinate, showed no evidence for the disappearance of a tyrosinate already existing in bR_{568}. Thus, while all of these results suggest that tyrosine plays a role in the proton pumping mechanism, the studies give no indication of the presence of a tyrosinate at pH 7 prior to light activation.

Additional experiments, however, suggest the presence of a tyrosinate in bR_{568}. FTIR and UV difference spectra have been interpreted to indicate deprotonation of a tyrosine in the conversion of bR_{555} to bR_{568} (Dollinger et al., 1986; Roepe et al., 1988), protonation of a tyrosinate during the bR_{568} to K phototransition (Dollinger et al., 1986, 1987; Rothschild, 1986; Rothschild et al., 1986; Roepe, 1987a,b), and deprotonation of a tyrosine between bR_{568} and M (Dollinger et al., 1986; Roepe et al., 1987a,b; Braiman et al., 1987). Subsequent studies of tyrosine mutants (Mogi et al., 1987) identify Tyr-185 as the amino acid residue that is altered in the $bR_{568} \rightarrow$ K and $bR_{568} \rightarrow$ M transitions (Braiman et al., 1988).

The existence of tyrosinate in bR_{568} (or bR_{555}) is a hypothesis that can be clearly and unambiguously tested by ^{13}C NMR. It has been known for many years that the ^{13}C chemical shifts of aromatic ring carbons of phenols depend strongly on whether the phenol is protonated or deprotonated. In particular, the isotropic shift of the carbon proximal to the hydroxyl group moves downfield by 8–12 ppm on deprotonation. For example, results from ^{13}C solution NMR show a 10.4 ppm shift change upon deprotonation of a tyrosyl residue in a small peptide (Norton & Bradbury, 1974). Using solid-state ^{13}C NMR, we show here that a similar change (10–14 ppm) is observed in the isotropic shift of several model compounds, with the change concentrated primarily in the σ_{22} tensor element (30–40 ppm). A variety of model compounds were studied, including *p*-nitrophenol and its sodium salt, *p*-cresol and its sodium and potassium salts, and tyrosine and tyrosine ethyl ester.

Partial titration of the tyrosine ^{13}C NMR resonances of a protein was first attempted by Maurer et al. (1974) for BPTI. However, complete titration was first accomplished by Wilbur and Allerhand (1976), who showed in several myoglobins that "surface" tyrosines gave pK's close to those of free tyrosine and small tyrosine-containing peptides in solution (p$K_a \simeq 10$), while "buried" tyrosines were essentially "untitratable" (p$K_a > 12.5$). Those tyrosinates that were formed showed isotropic shifts approximately 9.6–11.2 ppm downfield from those of protonated tyrosine. These studies were carried out via solution NMR methods, which in general have not been successfully applied to bR. However, solid-state NMR techniques provide high-resolution spectra of intact, fully hydrated purple membrane (Harbison et al., 1984a,b, 1985a; deGroot et al., 1988, 1989; Smith et al., 1989a,b; Engelhard et al., 1989). The present work reports the application of these methods to [4′-^{13}C]Tyr-bR, and in addition, difference spectra are utilized to help distinguish the labeled tyrosine signal from the natural abundance ^{13}C signals. In contrast to the FTIR results, we find no evidence for tyrosinate in fully hydrated, dark-adapted bR, at ambient or low temperature. The chemical shifts of all the tyrosines in bR are essentially invariant between pH 2 and pH 10, and only small changes occur as high as pH 12. At pH 13, where the protein begins to denature (Druckmann et al., 1982), tyrosinate formation is observed. Therefore, there is no evidence for tyrosinates in bR_{568} or bR_{555}.

Materials and Methods

Preparation of Model Compounds. L-Tyrosine hydrochloride was obtained by dissolving L-tyrosine in hot 5 N HCl and cooling to 0 °C. L-Tyrosine ethyl ester was purchased from Sigma Chemical Co. (St. Louis, MO) and used without further purification. Sodium and potassium cresolates were prepared from *p*-cresol by addition of equimolar quantities of sodium hydroxide or potassium hydroxide, respectively, in aqueous solution followed by evaporation of the water. The cresolates were washed in dry ether and kept under vacuum for 2 h before use. Sodium tyrosinate was made by addition of sodium hydroxide solution to an aqueous solution of tyrosine. Crystals did not form readily so the solution was evaporated to dryness. The simple dipeptides L-Leu-L-Tyr and L-Tyr-L-Phe were purchased from Sigma and used without further purification.

The *p*-nitro[1-^{13}C]phenol was synthesized from [2-^{13}C]-acetone (Cambridge Isotope Laboratories, Woburn, MA). The acetone was condensed with sodium nitromalonaldehyde following the procedure given by Drehman et al. (1961). The labeled *p*-nitrophenol was purified by chromatography on silica gel (E. Merck), with ether–petroleum ether (3:7 v/v) as eluant. Sodium *p*-nitro[1-^{13}C]phenolate was prepared by the reaction of equimolar quantities of *p*-nitro[1-^{13}C]phenol and sodium hydride in solution with dry tetrahydrofuran under argon. Cold solutions of the two reactants were added slowly under stirring. The solution was left for 12 h at room temperature and then evaporated to dryness under vacuum. The dry red mass was recrystallized from water to produce *p*-nitro[1-^{13}C]phenolate tetrahydrate.

Preparation of [4′-^{13}C]Tyrosine. The [4′-^{13}C]Tyr used to biosynthetically label bR was prepared from [1-^{13}C]phenol by use of the β-tyrosinase activity of *Erwinia herbicola* (Enei et al., 1973). The [4′-^{13}C]Tyr was purified by recrystallization from water, and characterized by ^1H NMR.

The [1-^{13}C]phenol was synthesized from the *p*-nitro[1-^{13}C]phenol, which was prepared as described above. The purified nitrophenol was methylated and reduced to [1-^{13}C]-anisidine by the method of Viswanatha and Hruby (1979). The anisidine was dissolved in 3 M HCl, cooled to 0 °C, and then diazotized with a solution of sodium nitrite at 0–4 °C for 1 h. The resulting diazonium chloride was then treated with 50% hypophosphorous acid and kept in the cold for 4–5 days. Evolution of nitrogen was profuse during the first 24 h. The labeled anisole was extracted with ether, purified by column chromatography over silica, and eluted with pentane. The solvent was evaporated carefully in a Vigreux column. The anisole was characterized by ^1H and ^{13}C NMR and then demethylated with a solution of BBr_3 in methylene chloride. The [1-^{13}C]phenol was extracted with the same solvent and washed with a saturated solution of sodium chloride. After careful evaporation of the solvent, the labeled phenol was

purified by chromatography over silica with petroleum ether–ether (9:1 v/v) as eluant. It was characterized by ^{1}H and ^{13}C NMR.

The method described here for the preparation of phenol from nitrophenol utilizes methylation of the hydroxyl group for protection during diazotization. Walker et al. (1986) and Winkel et al. (1989) have subsequently succeeded in directly diazotizing the unprotected *p*-aminophenol.

Preparation of bR Samples. The labeled tyrosine was incorporated into purple membrane by growing *Halobacterium halobium* (JW-3) in a defined medium similar to that of Gochnauer and Kushner (1969) except that all D-amino acids and NH_4Cl were removed and all L-Tyr was replaced with a quarter as much L-[4′-^{13}C]Tyr and a trace amount of L-[2′,6′-$^{3}H_2$]Tyr for monitoring incorporation. The purple membrane was isolated by the method of Oesterhelt and Stoeckenius (1974) and analyzed by ammonia acetone extraction and by amino acid analysis. Over 80% of the radioactivity was found in tyrosine, and the specific activity indicated that the tyrosines were about 60% labeled.

The bR was titrated in two different ways. In the first, purple membrane was washed and suspended in buffers covering the pH range of 1.95–11.2. In the second, purple membrane was suspended in deionized water, and the pH was raised from 7 to 13 with additions of small amounts of 5×10^{-2} N sodium hydroxide.

Buffers used for the pH titration were 100 mM phosphate (pH 7.2), 100 mM borate (pH 9.22 and 10.15), 100 mM carbonate (pH 11.2), and 100 mM oxalate (pH 4.45 and 1.95); the sodium salts were used in all cases. For the buffered series, 80 mg of purple membrane was, in each case, washed once with 5 mL of distilled water, washed twice with the same volume of the appropriate buffer, and finally pelleted for 2 h at 20000*g*.

For the unbuffered series 35–60 mg of purple membrane was suspended in 35 mL of deionized water, and the pH was raised to 10.0, 10.9, 12.0, and 12.9 with 10^{-4} to 5×10^{-2} N sodium hydroxide. The buffering capacity of the protein was taken into consideration by allowing the pH to equilibrate (approximately 5 min) after the addition of sodium hydroxide. The suspensions were pelleted for 2 h at 20000*g*. The pH of the supernatant was measured in each case to ensure that it had not changed significantly. The pH of the supernatants did not differ by more than 0.2 pH unit from that of the original suspensions. However, because of this modest variability of the pH values for this unbuffered titration, we report only two significant digits for the pH.

At each pH, absorption spectra were run immediately, after several hours, and after 1 day to monitor the integrity of the protein. The ratio of the absorbance at 280 nm to that at 560 nm was used as a measure of denaturation or bleaching of the protein. On the basis of UV/vis spectra, the sample titrations appear to be reversible for pH <13 and irreversible for pH >13.

NMR Spectroscopy. In each case, the bR pellet was transferred to a 7-mm cylindrical single-crystal sapphire rotor (Doty Scientific, Columbia, SC). MAS NMR spectra were obtained at a field of 7.4 T (^{13}C and ^{1}H frequencies of 79.9 and 317.6 MHz, respectively), from a standard cross-polarization pulse sequence (Pines et al., 1973) with a mix time of 2 ms, sample rotation rates of 2–5 kHz, and a decoupling field equivalent to 100 kHz. Use of a spinning speed controller (deGroot et al., 1988) held the speed of each sample fixed within ±5 Hz during the 6–12 h of data collection, permitting accurate subtractions of the natural abundance background for difference spectra. The magic angle was checked periodically with an enriched glycine sample. Acquisition time varied from 10 to 40 ms, and typically, 20000 transients were accumulated per purple membrane spectrum and considerably fewer for model compounds. Recycle delays were 2 s for bR, ~10 s for crystalline tyrosine derivatives, and 100–200 s for cresol, cresolates, nitrophenol, and nitrophenolate. In each case the recycle delay was adequate to allow full relaxation (>5 ^{1}H T_1's). The C-1 resonances of the cresol and cresolates were assigned by use of a delay without decoupling to suppress the signal of protonated carbons (Opella & Frey, 1979; Munowitz et al., 1981). All isotropic shifts were referenced to external TMS. For the bR spectra we used a natural abundance background peak positioned at 55.8 ppm (relative to external TMS) as an internal calibration standard. This peak position is invariant with temperature and pH. The principal values of the chemical shielding tensors for the buffered bR samples and the model compounds were calculated from the sideband patterns at a minimum of two distinct spinning speeds in the range of 2.0–2.5 kHz by the method of Herzfeld and Berger (1980), using the CERN (Geneva) MINUIT fitting package (deGroot et al., 1989). For the unbuffered series, a spinning speed of 2.5 and/or 4.0 kHz was used.

Spectra of the buffered samples were obtained at room temperature. To check for any irreversible changes in the protein, a spectrum at pH 7.2 was obtained both after the pH 2.0 spectrum and after the pH 11.0 spectrum had been obtained. In both cases, there were no changes in the pH 7.2 spectrum.

Spectra of the unbuffered samples were obtained at room temperature and at low temperatures, cold (−20 to −90 °C) nitrogen gas being used to spin the sample (F. Creuzet, H. J. M. deGroot, P. J. Allen, and R. G. Griffin, unpublished results). The low temperatures freeze out any dynamic behavior of the tyrosine residues and ensure that they cross-polarize uniformly. No differences were seen in the tyrosine signal between the spectra of the room temperature buffered samples and of cold unbuffered samples. (Slight differences in the alkyl region are seen between room temperature and frozen spectra.) Difference spectra were obtained by subtracting the spectrum of a natural abundance (unlabeled) bR sample from each of the spectra of [4′-^{13}C]Tyr-bR. The intensity and phase of the labeled bR spectrum were adjusted so as to provide the optimal subtraction of the natural abundance background signal in the labeled spectrum. This method permitted observation of the signal due only to the label and would therefore reveal any change in intensity which might occur in the region of the natural abundance carbonyl signal. The unlabeled spectrum was collected at the same temperature and spinning speed as the labeled spectra. The pH of the unlabeled sample was not varied.

To compensate for varying sample size from one pH to the next, the intensity of each spectrum before subtraction was adjusted to match the natural abundance background signal, and the same unlabeled bR spectrum was subtracted from each. When analyzed in this fashion, the total integrated intensity of the lines in each difference spectrum is essentially constant.

Results

In solid-state ^{13}C NMR spectra obtained for several model compounds, the isotropic chemical shift of the carbon proximal to the hydroxyl group moves downfield 10–14 ppm upon deprotonation of the hydroxyl group. Figure 1 shows spectra of *p*-nitro[1-^{13}C]phenol and sodium *p*-nitro[1-^{13}C]phenolate tetrahydrate. In addition to the downfield shift of the 1-^{13}C

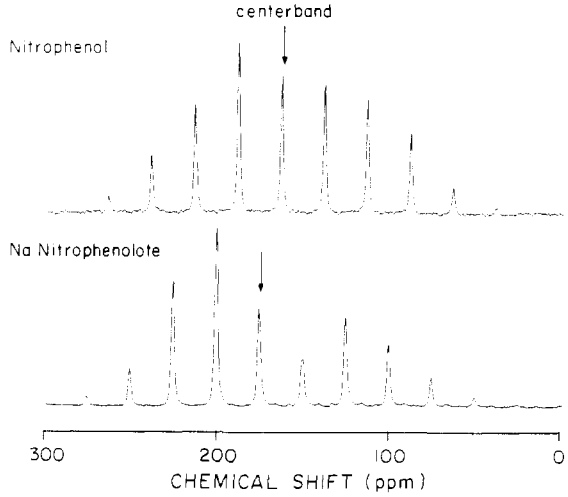

FIGURE 1: (Top) 79-MHz ^{13}C MAS spectrum of *p*-nitro[1-^{13}C]phenol in which the only signal visible is due to the labeled carbon proximal to the hydroxyl group. (Bottom) Spectrum of *p*-nitro[1-^{13}C]phenolate tetrahydrate, illustrating the shift of 11 ppm that occurs on deprotonation of the ^{13}C–OH. The shift is localized primarily in the σ_{22} element of the tensor (see Figure 2). Spectra were taken at room temperature with a spinning speed of 2 kHz.

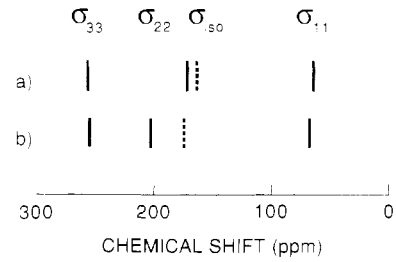

FIGURE 2: ^{13}C chemical shift tensor elements (|) and isotropic chemical shifts (:) for the model compounds (a) *p*-nitrophenol and (b) *p*-nitrophenolate tetrahydrate. The σ_{11} and σ_{33} tensor elements are insensitive to protonation state, whereas the σ_{22} element moves downfield for the deprotonated species.

centerband, we see the sideband intensity pattern is altered upon deprotonation. As shown in Table I and Figure 2, this is a result of a large change in the σ_{22} tensor element (37 ppm), with only minor changes (1–2 ppm) in the σ_{11} and σ_{33} elements.[3] A similar effect is seen in the cresol model compounds (Table I).

Table I also includes the shift tensor elements for [4′-^{13}C]Tyr-bR at various pHs. This shift tensor information was obtained from difference spectra as illustrated in Figure 3. Figure 3 (top) shows a spectrum of [4′-^{13}C]Tyr-bR taken at pH 6.8. This spectrum contains signal due to natural abundance ^{13}C, in addition to signals due to the isotopically labeled tyrosine residues. Figure 3 (middle) shows a spectrum of an unlabeled bR sample (i.e., only the natural abundance ^{13}C signal) obtained at the same spinning speed. The natural abundance spectrum shows the characteristic lines due to carboxyl groups around 176 ppm and the signal arising from alkyl carbons further upfield. Subtraction of the unlabeled spectrum from the labeled spectrum yields the difference spectrum shown at the bottom, which contains signals due solely to the 11 ^{13}C-labeled tyrosine residues in bR.

Figure 4 shows difference spectra obtained in a similar manner at pH 7, 10, 12, and 13. The difference spectra taken at pH values between 2 and 7 (not shown) as well as those taken between pH 7 and pH 12 exhibit essentially a single signal for which the centerband is at 156.5 ppm. For spectra taken at the same spinning speed, the sidebands display a similar intensity pattern, indicating that the shift tensor elements have similar values in the pH range from 2 to 12.

[3] We have also seen multiple crystal forms of the anhydrous sodium *p*-nitro[1-^{13}C]phenolate, before recrystallization in water, which differed in their σ_{22} tensor elements.

Table I: Isotropic and Anisotropic Chemical Shifts of the ^{13}C–OH/^{13}C–O$^-$ Carbons of Model Phenol/Phenolate and Tyrosine Compounds and [4′-^{13}C]Tyr-bR[a]

	σ_i	σ_{11}	σ_{22}	σ_{33}
cresol	152.4	62	158	238
potassium cresolate	166.1	61	204	233
sodium cresolate	165.2	56	202	238
nitrophenol	164.5	63	172	258
sodium nitrophenolate tetrahydrate[b]	176.3	64	209	256
Tyr-HCl	152.6	59	158	241
tyrosine ethyl ester	156.2	61	163	245
tyrosine ethyl ester hydrochloride	158.0	56	167	252
tyrosine	155.8	64	157	247
sodium tyrosinate	165.4	66	186	244
L-Leu-L-Tyr	153.5	63	151	247
L-Tyr-L-Phe·H_2O	156.0	57	163	248
bR, pH 4.45	156.2	73	158	238
bR, pH 7	156.5	66	159	245
bR, pH 10	156.1	65	159	244
bR, pH 13, Tyr	156.6	69	158	243
bR, pH 13, Tyr$^-$	164.9	67	182	246

[a] All shifts are referenced to external TMS. Typical errors for the isotropic (σ_i) and anisotropic (σ_{ii}) chemical shifts are ±0.2 ppm and ±5 ppm, respectively. For the bR samples, where some heterogeneity is present, shifts are given for the dominant peak. [b] See text footnote 3.

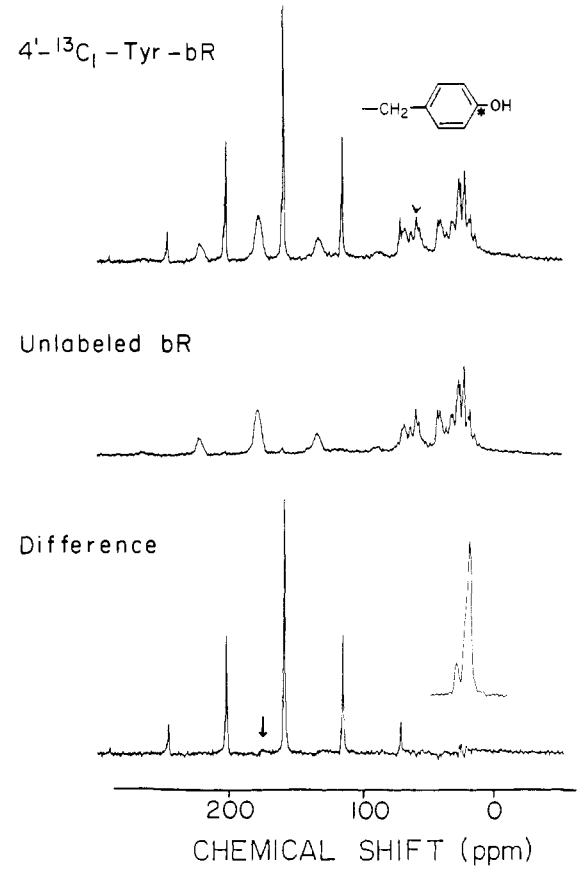

FIGURE 3: 79-MHz solid-state ^{13}C spectra of dark-adapted [4′-^{13}C]Tyr-bR at pH 6.8 (top) and of natural abundance bR (middle) and the difference spectrum resulting from appropriate scaling and subtraction (bottom). Spectra were taken at 3.5 kHz and 20 °C and result from accumulation of approximately 20 000 transients. The anticipated position for a tyrosinate centerband is indicated with an arrow. Inset spectrum above the difference spectrum is an expanded (five times) centerband showing the structure that we presume to be due to heterogeneity in the chemical environment of the Tyr's in bR.

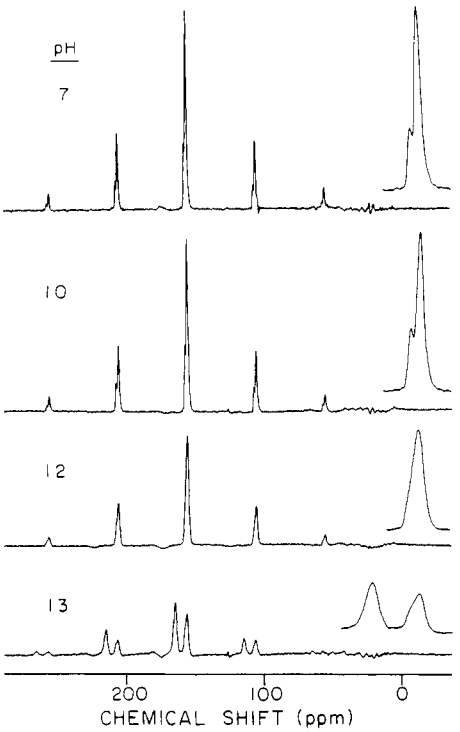

FIGURE 4: Difference spectra for [4′-^{13}C]Tyr-bR obtained as described in the caption for Figure 3; the ^{13}C-labeled sample was adjusted to pH values of 7, 10, 12, and 13 for the four spectra (top to bottom). All spectra were taken at ca. −40 °C and a spinning speed of 4 kHz. Inset spectra are expanded (five times) centerband regions. At pH 13, approximately half of the tyrosines appear to be deprotonated, as indicated by the intensity at 175 ppm where the deprotonated Tyr signal is expected. Comparison of the pH 13 spectrum with those taken at pH 7–12 clearly shows that no tyrosinates are observable at or below pH 12.

Comparison with the model compound data in Table I indicates that the bR signal for pH ≤12 is due to protonated tyrosine residues.

A closer examination of the expanded centerband, shown in the inset on the right side of the pH 7 spectrum in Figures 3 and 4, reveals a shoulder which is approximately 2 ppm downfield of the primary tyrosine line. The integrated intensity of this peak is ~20% of the total integrated intensity of the main tyrosine signal, suggesting it is due to 2 of the 11 tyrosines in bR which reside in slightly different environments, perhaps due to H-bonding. In proteins with multiple Tyr residues, it is quite common to see a dispersion in 4′-^{13}C chemical shifts of a few ppm (Wilbur & Allerhand, 1976). In bR, a protein with 11 Tyr's, it is perhaps surprising that there is not a larger inequivalence, and therefore more structure, in the Tyr line. The shift difference is too small to be interpreted as ionization of a tyrosine residue, except in an unusual situation where the equilibrium would be shifted heavily toward the protonated form and be independent of pH, as discussed below.

The difference spectrum obtained at pH 13 is shown at the bottom of Figure 4. It is only under such extreme conditions, when the protein starts to denature, that intensity is observed at 9 ppm downfield. On the basis of the isotropic shift at 165 ppm and the values of the tensor elements (see Table I), we assign this line to deprotonated tyrosine residues. The integrated intensities of the lines indicate that at pH 13 approximately 6 of the 11 tyrosines are deprotonated.

In addition to the emergence of a tyrosinate line in the pH 13 spectrum, more subtle changes are noted in the difference spectra with increasing pH. We observe line broadening from ~1.0 ppm at pH 7 to ~2.0 ppm at pH 12 and 13. (See expanded centerbands in the insets on the right side of Figure 4.) This broadening conceals the tyrosine heterogeneity which is observed in the pH 7 and 10 spectra.

As mentioned above, the intensities of the spectra were adjusted before subtraction so as to make the signal due to natural abundance background identical for each pH. This approach compensated for varying sample size and calibrated the spectra so that the intensities of the difference spectra in Figure 4 are directly comparable to one another. We find that the total integrated intensity of the tyrosine signal in each spectrum is approximately the same. The lower peak heights reflect the broader line widths at higher pH.

Finally, we should mention that the spectra shown in Figures 3 and 4 have been reproduced with four different samples and under a variety of experimental conditions, i.e., temperature, cross-polarization times, and rf field strength. The low temperatures are particularly important, since here the motion of the tyrosines is frozen out and all 11 residues can be expected to be cross-polarized uniformly (Kinsey et al., 1981). In no case have we found lines in the spectral region where tyrosinate is expected.

Discussion

Protonation/Deprotonation Effects on Phenolic Chemical Shielding Tensors. Salts of tyrosine with strong bases do not crystallize readily from aqueous solution, and therefore, samples were prepared by evaporation of solutions of tyrosine at high pH. We also examined *p*-cresol and its sodium and potassium salts as representatives of a phenolic acid/conjugate base pair. The similarity between the *p*-cresol 1-C tensor and the corresponding 4-C tensors of tyrosine hydrochloride and tyrosine ethyl ester justifies the use of *p*-cresol as a model (see Table I). The chemical shielding tensors obtained from tyrosine and sodium tyrosinate are also reported in Table I, despite the fact that the latter was not highly crystalline.

The cresolate data show that the deprotonation effect observed at 1-C in solution NMR spectra is reproduced in the solid state. Furthermore, the downfield shift is a result of an ~40 ppm shift in the σ_{22} element of the shielding tensor, with little effect on the other two tensor elements. This element has been assigned to the direction in the plane of the aromatic ring, perpendicular to the C–O bond (Pausak et al., 1973; Veeman, 1981). Such localized changes in shift tensors have been noted in the past (Pines et al., 1973; Harbison et al., 1985a,b; Mehring et al., 1982, Terao et al., 1984; deGroot et al., 1989) and may indeed prove to be the rule rather than the exception.

In nitrophenol the isotropic shift and shift tensor elements are about 9 ppm downfield from the corresponding elements for tyrosine. This is due to the effect of the nitro group, which extends the conjugated system and alters the electron density at the hydroxyl carbon. However, nitrophenol displays a similar change in σ_{22} upon deprotonation. For this reason, we included *p*-nitrophenol and sodium *p*-nitrophenolate with our other model compounds.

We also include in Table I the chemical shift tensors for the 4′-carbon of Tyr in two simple unlabeled dipeptides, L-Leu-L-Tyr and L-Tyr-L-Phe. The similarity of the shift tensors to that of Tyr implies that crystal packing and other intermolecular interactions do not drastically affect the tensors in the simple model compounds. Furthermore, it demonstrates that substituent effects are not important and hence that simple phenols are good model compounds.

^{13}C Chemical Shifts of [4′-^{13}C]Tyr-bR. Figure 3 shows the pH 6.8 ^{13}C MAS spectra of [4′-^{13}C]Tyr-bR and unlabeled bR, and the difference between the two. The intense downfield resonance deriving from the 11 ^{13}C-labeled tyrosine residues

is quite apparent. Figure 4 shows the −50 to 300 ppm region of difference spectra obtained in a manner similar to that illustrated in Figure 3. In the pH 7 spectrum, the only significant resonances lie in the 156–158 ppm region, where the signals of protonated tyrosines fall. There are no additional peaks around 165–167 ppm, the expected resonance position of a deprotonated tyrosine. Furthermore, none of the difference spectra obtained at pH values between 2 and 12 (Figure 4 and data not shown) contain any resonances that could be attributed to tyrosinate. Finally, the principal values of the shielding tensors derived from rotational sideband intensities of the spectra taken at pH values of between 2 and 12 correspond closely with those of the protonated tyrosines (Table I). Thus, we see no evidence for a tyrosinate in dark-adapted bR within 5 pH units on either side of neutrality. On the other hand, at pH 13 (see also Figure 4), we do observe an additional line at 165 ppm that corresponds to deprotonation of 6 out of the 11 tyrosine residues in bR. This observation demonstrates the ability to detect tyrosinates in proteins by solid-state NMR.

The present NMR results are difficult to reconcile with FTIR and UV results, which have been interpreted as indicating the presence of tyrosinate (Dollinger et al., 1986; Rothschild, 1986; Rothschild et al., 1986; Roepe et al., 1987a,b, 1988; Braiman et al., 1987, 1988). We have systematically explored several experimental avenues—low temperatures where the interference of molecular motion with cross-polarization will be minimal and varied cross-polarization times, rf field strengths, sample pH, etc.—on multiple samples in an effort to detect a tyrosinate signal in dark-adapted bR. To date, the NMR spectral results have been highly reproducible and give no indication of the presence of a long-lived tyrosinate at pH $\lesssim$12. Thus, if tyrosinate occurs in bR_{568}, it must be rare or short-lived. One may envision three possibilities under which it would occur. (1) If only a small fraction of the bR_{568} molecules contain a tyrosinate, then this would be difficult to detect with the NMR. On the basis of preliminary studies of light-adapted samples (Thompson et al., 1990; A. E. McDermott, L. K. Thompson, M. R. Farrar, C. Winkel, S. K. Das Gupta, J. Lugtenburg, J. Herzfeld, and R. G. Griffin, unpublished results) that fraction would have to be very small and, therefore, might be of little significance for a pumping mechanism. (2) It is possible that bR_{568} in dark-adapted samples may differ from the bR_{568} in the light-adapted samples studied optically. In particular, it is possible that, if a Tyr^- were formed during the photocycle, it could reprotonate more slowly than the chromophore relaxes to the all-trans configuration. Thus, Tyr^- might still be detected in bR_{568} of photocycling samples but not in bR_{568} of static dark-adapted samples. Results of NMR experiments to be described in future publications indicate that the same argument would have to be applied to bR_{568} trapped at low temperatures in light-adapted samples (Thompson et al., 1990; McDermott et al., unpublished results). (3) It is possible that bR_{568} contains tyrosinate only for a small fraction of the time—i.e., that there is a tyrosine residue in rapid exchange between protonated and deprotonated states, with the equilibrium shifted toward the Tyr form. The shoulder shown in the inset of Figures 3 and 4 at 2 ppm below the main Tyr signal could possibly represent such a residue. The small shift from the main line dictates that the population of the deprotonated form be <20% and not change significantly over 5 pH units. As mentioned previously, it seems more likely that this shoulder is due to the dispersion of Tyr signals commonly observed in proteins with multiple tyrosine residues.

Our titration of dark-adapted bR indicates an apparent tyrosine pK of ~13, typical of buried residues. However, due to the net negative charge of the purple membrane, the pH at the membrane surface is lower than that in the bulk, to a degree that depends on the amount and type of salt in the solution. For the ionic condition that we have used (~100 mM monovalent electrolyte), the discrepancy may be on the order of 2 pH units (Szundi & Stoeckenius, 1989). Thus, it would be premature to deduce from our titration that the tyrosines of bR are all buried. Another titration in the presence of high concentrations of divalent cations would be required to obtain a better estimate of the pK's of the tyrosines in bR.

Conclusions

(1) Solid-state ^{13}C NMR data on a number of model compounds (including *p*-nitrophenol, sodium *p*-nitrophenolate tetrahydrate, *p*-cresol, sodium and potassium cresolates, tyrosine, sodium tyrosinate, tyrosine hydrochloride, L-tyrosine ethyl ester, L-Leu-L-Tyr, and L-Tyr-L-Phe) yield isotropic chemical shifts for the ^{13}C–OH/^{13}C–O^- in good agreement with solution NMR results. For each homologous pair, the phenoxide exhibits an isotropic chemical shift value 10–14 ppm downfield from the corresponding phenol; analysis of MAS sideband intensities indicates that these shifts arise from a 30–40 ppm downfield shift in the σ_{22} element of the shift tensor.

(2) The [4′-^{13}C]Tyr-bR samples prepared at pH 2–12 exhibit a single ^{13}C solid-state NMR resonance due to the labeled tyrosine and no signal attributable to tyrosinate. The tyrosine signal exhibits some structure, characterized by shifts of less than 2 ppm. We presume that this structure is due to heterogeneity in the chemical environment and not to deprotonation.

(3) At pH 13, a signal due to tyrosinate appears 9 ppm downfield from the tyrosine signal, with an amplitude corresponding to approximately half of the tyrosines present. Signal intensities indicate that the sensitivity for detection of a tyrosinate is comparable to that for a tyrosine and that within our current signal-to-noise ratio one-third of one tyrosinate per bR molecule would be detectable.

(4) Finally, we conclude that in dark-adapted bR there is less than one-third of one tyrosinate per bR molecule at pH values less than 12 and therefore that it is unlikely that either bR_{555} or bR_{568} contains a tyrosinate at pH values less than 12.

Registry No. Tyr, 60-18-4; [4′-^{13}C]Tyr, 81201-90-3; Tyr·HCl, 16870-43-2; Tyr ethyl ester, 949-67-7; Tyr ethyl ester hydrochloride, 4089-07-0; Tyr·Na, 16655-52-0; L-Leu-L-Tyr, 968-21-8; L-Tyr-L-Phe·H_2O, 88374-56-5; cresol, 1319-77-3; potassium cresolate, 12002-51-6; sodium cresolate, 34689-46-8; nitrophenol, 25154-55-6; sodium nitrophenolate tetrahydrate, 126901-46-0; [2-^{13}C]acetone, 3881-06-9; sodium nitromalonaldehyde, 126901-44-8; *p*-nitro[1-^{13}C]phenolate tetrahydrate, 126901-43-7; [1-^{13}C]phenol, 29809-11-8; *p*-nitro[1-^{13}C]phenol, 3881-07-0.

References

Argade, P. V., & Rothschild, K. J. (1983) *Biochemistry 22*, 3460–3466.

Bagley, K., Dollinger, G., Eisenstein, L., Singh, A. K., & Zimanyi, L. (1982) *Proc. Natl. Acad. Sci. U.S.A. 79*, 4972–4976.

Bayley, H., Huang, K.-S., Radhakrishnan, R., Ross, A. H., Takagaki, Y., & Khorana, H. G. (1981) *Proc. Natl. Acad. Sci. U.S.A. 78*, 2225–2229.

Becher, B., Tokunaga, F., & Ebrey, T. G. (1978) *Biochemistry 17*, 2293–2300.

Bogomolni, R. A. (1980) in *Bioelectrochemistry* (Keyzer, H., & Gutman, F., Eds.) pp 83–95, Plenum Press, New York.

Bogomolni, R. A., Stubbs, L., & Lanyi, J. K. (1978) *Biochemistry 17*, 1037–1041.
Braiman, M., & Mathies, R. (1980) *Biochemistry 19*, 5421–5428.
Braiman, M., & Mathies, R. (1982) *Proc. Natl. Acad. Sci. U.S.A. 79*, 403–407.
Braiman, M. S., Ahl, P. L., & Rothschild, K. J. (1987) *Proc. Natl. Acad. Sci. U.S.A. 84*, 5221–5225.
Braiman, M. S., Mogi, T., Stern, L. J., Hackett, N. R., Chao, B. H., & Khorana, H. G. (1988) *Proteins: Struct., Funct., Genet. 3*, 219–229.
deGroot, H. J. M., Copiê, V., Smith, S. O., Allen, P. J., Winkel, C., Lugtenburg, J., Herzfeld, J., & Griffin, R. G. (1988) *J. Magn. Reson. 77*, 251–257.
deGroot, H. J. M., Harbison, G. S., Herzfeld, J., & Griffin, R. G. (1989) *Biochemistry 28*, 3346–3353.
Dollinger, G., Eienstein, L., Lin, S.-L., Nakanishi, K., & Termini, J. (1986) *Biochemistry 25*, 6524–6533.
Dollinger, G., Eienstein, L., Lin, S.-L., Nakanishi, K., & Termini, J. (1987) in *Biophysical Studies of Retinal Proteins* (Ebrey, T. G., Frauenfelder, H., Honig, B., & Nakanishi, K., Eds.) pp 120–125, University of Illinois Press, Champaign, IL.
Drehman, V. U., Purschel, V., & Wauschkun, H. (1961) *J. Prakt. Chem 4*, 122–126.
Druckmann, S., Ottolenghi, M., Pande, A., Pande, J., & Callender, R. H. (1982) *Biochemistry 21*, 4953–4959.
Enei, H., Nakazawa, H., Okumura, S., & Yamada, H. (1973) *Agric. Biol. Chem. 37*, 725–735.
Engelhard, M., Hess, B., Emeis, D., Metz, G., Kreutz, W., & Siebert, F. (1989) *Biochemistry 28*, 3967–3975.
Fukumoto, J. M., Hanamoto, J. H., & El-Sayed, M. A. (1984) *Photochem. Photobiol. 39*, 75–79.
Gochnauer, M. B., & Kushner, D. J. (1969) *Can. J. Microbiol. 15*, 1157–1165.
Hanamoto, J. H., Dupuis, P., & El-Sayed, M. A. (1984) *Proc. Natl. Acad. Sci. U.S.A. 81*, 7083–7087.
Harbison, G. S., Herzfeld, J., & Griffin, R. G. (1983) *Biochemistry 22*, 1–5.
Harbison, G. S., Smith, S. O., Pardoen, J. A., Mulder, P. P. J., Lugtenburg, J., Herzfeld, J., Mathies, R., & Griffin, R. G. (1984a) *Biochemistry 23*, 2662–2667.
Harbison, G. S., Smith, S. O., Pardoen, J. A., Mulder, P. P. J., Lugtenburg, J., Herzfeld, J., Mathies, R., & Griffin, R. G. (1984b) *Proc. Natl. Acad. Sci. U.S.A. 81*, 1706–1709.
Harbison, G. S., Smith, S. O., Pardoen, J. A., Courtin, J. M. L., Lugtenburg, J., Herzfeld, J., Mathies, R. A., & Griffin, R. G. (1985) *Biochemistry 24*, 6955–6962.
Herzfeld, J., & Berger, A. E. (1980) *J. Chem. Phys. 73*, 6021–6030.
Hess, B., & Kushchmitz, D. (1979) *FEBS Lett. 100*, 334–340.
Hsieh, C.-L., Nagumo, M., Nicol, M., & El-Sayed, M. A. (1981) *J. Chem. Phys. 85*, 2714–2717.
Kalisky, O., Ottolenghi, M., Honig, B., & Korenstein, R. (1981) *Biochemistry 20*, 649–655.
Kinsey, R. A., Kintanar, A., & Oldfield, E. (1981) *J. Biol. Chem. 256*, 9028–9036.
Lewis, A., Spoonhower, J., Bogomolni, R. A., Lozier, R. H., & Stoeckenius, W. (1974) *Proc. Natl. Acad. Sci. U.S.A. 71*, 4462–4466.
Maurer, W., Haar, W., & Ruterjans, H. (1974) *Z. Phys. Chem. (Frankfurt/Main) 93*, 119–129.
Mehring, M., Weber, T., Muller, W., & Wagner, G. (1982) *Solid State Commun. 45*, 1079–1082.
Mogi, T., Stern, L. J., Hackett, N. R., & Khorana, H. G. (1987) *Proc. Natl. Acad. Sci. U.S.A. 84*, 5595–5599.
Munowitz, M. G., Griffin, R. G., Bodenhausen, G., & Huang, T. H. (1981) *J. Am. Chem. Soc. 103*, 2529–2533.
Nagle, J., & Morowitz, H. J. (1978) *Proc. Natl. Acad. Sci. U.S.A. 75*, 298–302.
Nagle, J., & Tristan-Nagle, S. (1983) *J. Membr. Biol. 74*, 1–14.
Nagle, J. F. (1987) *J. Bioenerg. Biomembr. 19*, 413–426.
Norton, R. S., & Bradbury, J. H. (1974) *J. Chem. Soc., Chem. Commun.*, 870–871.
Oesterhelt, D., & Stoeckenius, W. (1973) *Proc. Natl. Acad. Sci. U.S.A. 70*, 2853–2857.
Oesterhelt, D., & Stoeckenius, W. (1974) *Methods Enzymol. 31*, 667–678.
Opella, S. J., & Frey, M. H. (1979) *J. Am. Chem. Soc. 101*, 5854–5856.
Pausak, S., Pines, A., & Waugh, J. S. (1973) *J. Chem. Phys. 59*, 591–595.
Pettei, M. J., Yudd, A. P., Nakanishi, K., Henselman, R., & Stoeckenius, W. (1977) *Biochemistry 16*, 1955–1959.
Pines, A., Gibby, M. G., & Waugh, J. S. (1973) *J. Chem. Phys. 59*, 569–590.
Roepe, P., Ahl, P. L., Das Gupta, S. K., Herzfeld, J., & Rothschild, K. J. (1987a) *Biochemistry 26*, 6696–6707.
Roepe, P., Scherrer, P., Ahl, P. L., Das Gupta, S. K., Bogomolni, R. A., Herzfeld, J., & Rothschild, K. J. (1987b) *Biochemistry 26*, 6708–6717.
Roepe, P. D., Ahl, P. L., Herzfeld, J., Lugtenburg, J., & Rothschild, K. J. (1988) *J. Biol. Chem. 263*, 5110–5117.
Rosenbach, V., Goldberg, R., Gilon, C., & Ottolenghi, M. (1982) *Photochem. Photobiol. 36*, 197–201.
Rothschild, K. J. (1986) *Methods Enzymol. 127*, 343–353.
Rothschild, K. J., Argade, P. V., Earnest, T. N., Huang, K.-S., London, E., Liao, M.-J., Bayley, H., Khorana, H. G., & Herzfeld, J. H. (1982) *J. Biol. Chem. 257*, 8592–8595.
Rothschild, K. J., Roepe, P., Ahl, P. L., Earnest, T. N., Bogomolni, R. A., Das Gupta, S. K., Mulligen, C. M., & Herzfeld, J. (1986) *Proc. Natl. Acad. Sci. U.S.A. 83*, 347–351.
Scherrer, P., & Stoeckenius, W. (1984) *Biochemistry 23*, 6195–6202.
Scherrer, P., & Stoeckenius, W. (1985) *Biochemistry 24*, 7733–7740.
Scherrer, P., Mathew, M. K., Sperling, W., & Stoeckenius, W. (1989) *Biochemistry 28*, 829–834.
Smith, S. O., Pardoen, J. A., Mulder, P. P. J., Curry, B., Lugtenburg, J., & Mathies, R. (1983) *Biochemistry 22*, 6141–6148.
Smith, S. O., Myers, A. B., Pardoen, J. A., Winkel, C., Mulder, P. P. J., Lugtenburg, J., & Mathies, R. (1984) *Proc. Natl. Acad. Sci. U.S.A. 81*, 2055–2059.
Smith, S. O., Lugtenburg, J., & Mathies, R. A. (1985) *J. Membr. Biol. 85*, 95–109.
Smith, S. O., Courtin, J., van den Berg, E., Winkel, C., Lugtenburg, J., Herzfeld, J., & Griffin, R. G. (1989a) *Biochemistry 28*, 237–243.
Smith, S. O., de Groot, H. J. M., Courtin, J. M. L., Lugtenburg, J., Herzfeld, J., & Griffin, R. G. (1989b) *Biochemistry* (in press).
Stockburger, M., Alshuth, T., Oesterhelt, D., & Gartner, W. (1986) in *Spectroscopy of Biological Systems* (Clark, R. J. H., & Hester, R. E., Eds.) pp 483–547, Wiley, New York.
Stoeckenius, W., & Bogomolni, R. A. (1982) *Annu. Rev. Biochem. 51*, 587–616.

Szundi, I., & Stoeckenius, W. (1989) *Biophys. J. 56*, 369-383.
Terao, T., Maeda, S., Yamabe, T., Akagi, K., & Shirakawa, H. (1984) *Chem. Phys. Lett. 103*, 347.
Terner, J., & El-Sayed, M. A. (1985) *Acc. Chem. Res. 18*, 331-338.
Thompson, L. K., McDermott, A. E., Farrar, M. R., Griffin, R. G., Winkel, C., Lugtenburg, J., Brown, R. S., & Herzfeld, J. (1990) *Biophys. J. 57*, 364a.
Tsuda, M., Glaccum, M., Nelson, B., & Ebrey, T. G. (1980) *Nature (London) 287*, 351-353.
Veeman, W. S. (1981) *Philos. Trans. R. Soc. London A299*, 629-641.
Viswanatha, V., & Hruby, V. J. (1979) *J. Org. Chem. 44*, 2892-2896.
Walker, T. E., Matheny, C., Storm, C. B., & Hayden, H. (1986) *J. Org. Chem. 51*, 1175-1179.
Wilbur, D. J., & Allerhand, A. (1976) *J. Biol. Chem. 251*, 5187-5191.
Winkel, C., Aarts, M. W. M. M., van der Heide, F. R., Buitenhuis, E. G., & Lugtenburg, J. (1989) *Recl. Trav. Chim. Pays-Bas 108*, 139-146.
Zundel, G. (1988) in *Transport through Membranes: Carriers Channels, and Pumps* (Pullman, A., Ed.) pp 409-420, Kluwer Academic Publishers, Dordrecht, The Netherlands.

Structure of the Oligosaccharide of Hen Phosvitin As Determined by Two-Dimensional ^{1}H NMR of the Intact Glycoprotein†

Ron L. Brockbank and Hans J. Vogel*
Division of Biochemistry, Department of Biological Sciences, University of Calgary, Calgary, Alberta, Canada T2N 1N4
Received May 1, 1989; Revised Manuscript Received February 15, 1990

ABSTRACT: The major form of the oligosaccharide of hen phosvitin was studied with two-dimensional ^{1}H NMR of the intact glycoprotein. Its structure was determined from an analysis of the chemical shifts of the structural reporter groups, and it was further confirmed by comparison to several related model oligosaccharides. The oligosaccharide is N-linked and is present in a 1:1 stoichiometry to the protein. It has a complex type 1 triantennary structure with two NeuAcα2,6Galβ1,4GlcNAcβ1,2 arms linked to the Man-4 and Man-4′ and a third Galβ1,4GlcNAcβ1,4 arm attached to the Man-4. The oligosaccharide contains the common core sequence which is present in all N-linked glycoproteins [Manα1,3(Manα1,6)-Manβ1,4GlcNAcβ1,4GlcNAcβ1,N]. In the course of this study, we have found that unique spin systems for the GlcNAc and NeuAc are obtained for spectra recorded in 90% H_2O. Their NH peaks were assigned at low pH, and these assignments proved useful for confirming the identity of cross-peaks in the anomeric region. In addition, the protons of GlcNAc-1 could be correlated to the NH of the asparagine link. The cross-peak patterns determined in phase-sensitive 2D experiments for the H1,H2 protons have a different appearance for each type of monosaccharide, and this information was also used for making first-order assignments. A comparison with model compounds suggests that the solution conformation of the oligosaccharide is not affected by its attachment to the protein.

Phosvitin is a highly phosphorylated glycoprotein which is found in the lipovitellin complex in the egg yolks of fish and birds. In response to hormones, the protein is synthesized in the liver as part of the large vitellogenin precursor (Tata, 1976). The precursor is glycosylated at a number of sites and is phosphorylated in the liver, from where it is transported via the bloodstream to the developing embryo (Taborsky, 1983). The vitellogenin complex is subsequently taken up into the oocytes, and here it is cleaved by specific proteases into a number of proteins including phosvitin which contains a single glycosylated site. The characterization of a glycosylated peptide (Shainkin & Perlmann, 1971a,b) from hen phosvitin was carried out almost 20 years ago at a time when no extensive knowledge of the biosynthesis of these compounds was available (Kornfeld & Kornfeld, 1985). In view of our present understanding of N-linked oligosaccharide sequences, the structure obtained from this initial study contains a highly unusual core sequence, and no successful attempts have since been made to reexamine this structure. The amino acid sequence of the major form of phosvitin has been deduced from the DNA sequence (Byrne et al., 1984), and this confirmed that the protein sequence at the glycosylation site was -Asn-X-Ser- which is common to all N-linked glycoproteins.

We have been working on the assignment of the proton nuclear magnetic resonance (NMR)[1] spectra of phosvitin using two-dimensional NMR techniques in an attempt to learn more about the nature of this unusual polyelectrolyte protein. In the course of this work, we detected a number of well-resolved cross-peaks which could be attributed to the oligosaccharide portion of the protein. Vliegenthart et al. (1983) have developed a proton NMR method for determining the compositions, sequences, and anomeric linkages of complex oligo-

†Supported by the Medical Research Council of Canada. The NMR spectrometer used was purchased with funds provided by the Alberta Heritage Foundation for Medical Research (AHFMR). R.L.B. and H.J.V. are holders of a studentship and a scholarship, respectively, from the AHFMR.

[1] Abbreviations: COSY, correlated spectroscopy; NMR, nuclear magnetic resonance; DQF, double quantum filter; TQF, triple quantum filter; RECSY, relayed correlated spectroscopy; HOHAHA, homonuclear Hartmann-Hahn; NOESY, nuclear Overhauser enhancement spectroscopy; GlcNAc, *N*-acetylglucosamine; Man, mannose; Gal, galactose; NeuAc, neuraminic acid (sialic acid); H1, anomeric proton; H3a, axial H3 proton; TSP, sodium 3-(trimethylsilyl)propionate-*2,2,3,3-d*$_4$.

0006-2960/90/0429-5574$02.50/0